NKT Cells Coexpressing a GD2-Specific Chimeric Antigen Receptor and IL15 Show Enhanced *In Vivo* Persistence and Antitumor Activity against Neuroblastoma

Xin Xu[1], Wei Huang[1], Andras Heczey[1,2,3], Daofeng Liu[1], Linjie Guo[1], Michael Wood[1], Jingling Jin[1], Amy N. Courtney[1], Bin Liu[1], Erica J. Di Pierro[1], John Hicks[2], Gabriel A. Barragan[1], Ho Ngai[1], Yuhui Chen[4], Barbara Savoldo[4], Gianpietro Dotti[4], and Leonid S. Metelitsa[1,2,3]

Abstract

Purpose: Vα24-invariant natural killer T cells (NKT) are attractive carriers for chimeric antigen receptors (CAR) due to their inherent antitumor properties and preferential localization to tumor sites. However, limited persistence of CAR-NKTs in tumor-bearing mice is associated with tumor recurrence. Here, we evaluated whether coexpression of the NKT homeostatic cytokine IL15 with a CAR enhances the *in vivo* persistence and therapeutic efficacy of CAR-NKTs.

Experimental Design: Human primary NKTs were *ex vivo* expanded and transduced with CAR constructs containing an optimized GD2-specific single-chain variable fragment and either the CD28 or 4-1BB costimulatory endodomain, each with or without IL15 (GD2.CAR or GD2.CAR.15). Constructs that mediated robust CAR-NKT cell expansion were selected for further functional evaluation *in vitro* and in xenogeneic mouse models of neuroblastoma.

Results: Coexpression of IL15 with either costimulatory domain increased CAR-NKT absolute numbers. However, constructs containing 4-1BB induced excessive activation-induced cell death and reduced numeric expansion of NKTs compared with respective CD28-based constructs. Further evaluation of CD28-based GD2.CAR and GD2.CAR.15 showed that coexpression of IL15 led to reduced expression levels of exhaustion markers in NKTs and increased multiround *in vitro* tumor cell killing. Following transfer into mice bearing neuroblastoma xenografts, GD2.CAR.15 NKTs demonstrated enhanced *in vivo* persistence, increased localization to tumor sites, and improved tumor control compared with GD2.CAR NKTs. Importantly, GD2.CAR.15 NKTs did not produce significant toxicity as determined by histopathologic analysis.

Conclusions: Our results informed selection of the CD28-based GD2.CAR.15 construct for clinical testing and led to initiation of a first-in-human CAR-NKT cell clinical trial (NCT03294954).

Introduction

Recent clinical trials have demonstrated that T cells expressing CD19-specific chimeric antigen receptors (CAR) induce sustained complete responses in patients with B-cell malignancies, leading to recent FDA approval of CD19-specific CAR T-cell therapies (1–3). However, clinical results obtained using CAR-redirected immunotherapy for solid tumors have been largely disappointing (4, 5). Hence, there is an urgent need for alternative strategies that improve the efficacy of CAR-mediated cancer immunotherapy in a wider range of cancers.

CARs can be expressed in T-cell subsets with defined functions. For instance, CARs have been expressed in cytotoxic T lymphocytes (CTL) specific for viral antigens such as those derived from the Epstein–Barr virus (6). Infusion of CTLs expressing a GD2-specific CAR (GD2.CAR) derived from the 14G2a monoclonal antibody to children with neuroblastoma was proven safe and achieved complete tumor responses in 3 of 11 patients with refractory/relapsed disease evaluated in one study (7, 8). However, CAR-CTLs did not effectively infiltrate tumors or persist *in vivo*, observations that were associated with tumor recurrence or lack of objective responses in the majority of patients. An attempt to increase the affinity of GD2.CAR via mutation of 14G2a single-chain variable fragment (scFv) enhanced antitumor activity of CAR T cells against neuroblastoma xenografts, but also produced lethal central nervous system toxicity due to recognition of low GD2-expressing normal brain cells in mice (9). New lines of research are examining CAR-based therapies for neuroblastoma and other solid tumors using innate and innate-like lymphocytes with natural tumor-trafficking and tumor-targeting properties including NK (10), γδ T (11), and Vα24-invariant natural killer T (NKT) cells (12).

[1]Texas Children's Cancer Center, Department of Pediatrics, Baylor College of Medicine, Houston, Texas. [2]Department of Pathology and Immunology, Baylor College of Medicine, Houston, Texas. [3]Center for Cell and Gene Therapy, Baylor College of Medicine, Houston, Texas. [4]Lineberger Comprehensive Cancer Center, University of North Carolina at Chapel Hill, Chapel Hill, North Carolina.

Note: Supplementary data for this article are available at Clinical Cancer Research Online (http://clincancerres.aacrjournals.org/).

Corresponding Author: Leonid S. Metelitsa, Department of Pediatrics, Baylor College of Medicine, 1102 Bates Avenue, C.1760.06, Houston, TX 77030. Phone: 832-824-4395; Fax: 832-825-4276; E-mail: lsmeteli@txch.org

Clin Cancer Res 2019;25:7126–38

doi: 10.1158/1078-0432.CCR-19-0421

Translational Relevance

Chimeric antigen receptor (CAR)–redirected T-cell adoptive immunotherapy remains largely ineffective in solid tumors due in part to the limited ability of conventional T cells to localize to and survive in tumor tissues. In this work, we exploit the intrinsic tumor-trafficking properties of natural killer T (NKT) cells to home to neuroblastoma tumors and target them with an engineered GD2-specific CAR coexpressing human IL15 to enhance CAR-NKT survival. We expressed a set of optimized GD2-based CAR constructs with either the human CD28 or 4-1BB costimulatory endodomain—each with or without IL15—in primary human NKTs and compared the therapeutic potential and toxicity of resultant CAR-NKTs. The results of this study informed the design of an ongoing first-in-human clinical evaluation of CAR-NKT cell therapy in children with neuroblastoma (NCT03294954).

NKTs are an evolutionarily conserved sublineage of innate-like T cells that express the Vα24-Jα18 invariant TCR α-chain and are characterized by reactivity to self- and microbial-derived glycolipids presented by the monomorphic HLA class-I–like molecule CD1d (13). Although the majority of solid tumors are CD1d-negative, the antitumor potential of NKTs has been demonstrated in numerous cancer models (13). We have reported that NKTs actively localize to tumors in response to tumor-derived chemokines CCL2 and CCL20 and that the presence of NKTs within the primary tumor site is associated with improved outcomes in children with neuroblastoma (14, 15). We have also shown that NKTs can be isolated from the peripheral blood, transduced with CARs, and expanded to clinical scale for adoptive cell therapy applications (12, 16).

CD19-specific CAR T cells with either CD28 or 4-1BB endodomains have been shown to be effective in patients with B-cell malignancies (2). In neuroblastoma patients, a GD2-specific CAR containing both CD28 and OX40 endodomains enhanced CAR T-cell expansion in the peripheral blood compared with a CAR without costimulation, but the magnitude of expansion was still limited (17). Furthermore, Long and colleagues reported that unlike CD19-specific CARs, GD2.CARs undergo tonic signaling resulting from spontaneous dimerization caused specifically by the 14G2a scFv. This unintended signaling, which led to early exhaustion of GD2.CAR T cells, was exacerbated in CARs containing the CD28 endodomain and attenuated in CARs containing 4-1BB (18).

We recently described a modified GD2.CAR containing a truncated form of the 14G2a heavy chain variable domain that despite retaining CD28 induces minimal tonic signaling and mediates enhanced antitumor activity in transduced T cells compared with the original GD2.CAR (19). In the same study, we also demonstrated that inclusion of IL15 in the optimized construct further enhanced the *in vitro* functionality and *in vivo* therapeutic potency of CAR.GD2 T cells in neuroblastoma models.

Mouse studies and *in vitro* human experimental models have both highlighted the central role of IL15 in NKT cell development and homeostatic maintenance (20, 21). Importantly, IL15 protects human NKTs from hypoxia, and transgenic expression of IL15 in adoptively transferred NKTs significantly enhances their antitumor activity (15). Therefore, we hypothesized that coexpressing IL15 with an optimized GD2.CAR would enhance the survival and antitumor effector functions of NKTs within neuroblastoma tissues leading to sustained tumor control. Our results reveal that GD2.CAR constructs encoding 4-1BB, but not CD28, costimulation triggered excessive activation-induced cell death (AICD) in NKTs during *in vitro* expansion. Importantly, coexpression of IL15 with the GD2.CAR containing the CD28 costimulatory endodomain increased the *in vivo* persistence and antitumor efficacy of CAR-NKTs in metastatic neuroblastoma models without causing evident toxicity. These preclinical assessments were instrumental in the implementation of first-in-human CAR-NKT clinical testing (NCT03294954).

Materials and Methods

Cell lines and culture conditions

CHLA-255, CHLA-136, LA-N-1, and LA-N-6 cell lines were established and maintained as previously described (15, 22, 23) and as detailed in Supplementary Methods. 293T cells were obtained from the ATCC. All cell lines were STR fingerprinted at MD Anderson Cancer Center within 1 year of use and regularly validated to be free of *Mycoplasma*.

NKT cell isolation, expansion, and transduction

NKT cells were isolated from healthy human donor peripheral blood, *ex vivo* expanded, and transduced with retroviral vectors encoding CAR constructs as previously described (24).

CAR constructs and retroviral vector production

SFG retroviral vectors were constructed as previously described (19) and used to produce retroviral supernatants. Retroviral supernatants were produced by transfecting 293T cells with a combination of an anti-GD2 CAR-containing plasmid, the RDF plasmid encoding the RD114 envelope, and the PeqPam3 plasmid encoding the MoMLV *gag-pol* as previously described (25). GeneJuice reagent (Novagen) was used to assist with transfection. Viral supernatants were collected after 48 and 72 hours, filtered with 0.45 μm filters, and frozen.

Flow cytometry

Immunophenotyping was performed using the monoclonal antibodies (mAb) and reagents detailed in Supplementary Methods. GD2.CARs were detected with the 14G2a anti-idiotype 1A7 mAb. Analysis was performed on an LSR-II 5-laser flow cytometer (BD Biosciences) using BD FACSDiva software version 6.0 and FlowJo 10.1 (Tree Star). SPICE software was used to evaluate the expression of exhaustion markers (26).

Cytotoxicity assays

Short-term cytotoxicity of parental and GD2.CAR NKTs against CHLA-255, CHLA-136, LA-N-1, and LA-N-6 cells was evaluated using a 4-hour luciferase assay as previously described (16). The calcein-AM M2 macrophage cytotoxicity assay was performed as previously described (27) and detailed in the Supplementary Methods. For the long-term cytotoxicity assay, GFP-tagged CHLA-255, CHLA-136, and LA-N-1 cells were plated in a 24-well plate 1 day prior to adding NKT cells at a 1:1 effector-to-target ratio. IL2 (50 U/mL) was added every other day. Cells were quantified by flow cytometry at day 7 based on NKT-invariant TCR and GFP expression, respectively, with nontransduced NKTs as negative controls.

Serial tumor challenge assay

CHLA-255, LA-N-1, and CHLA-136 cells were each cocultured with GD2.28z or GD2.28z.15 NKTs in a 24-well plate using fresh culture medium with 50 U/mL IL2. Five days later, cells were harvested, quantified using the trypan-blue exclusion methods, and analyzed for NKT and neuroblastoma cell markers by flow cytometry. CAR-NKT cells were then replated at a 1:1 E:T ratio with fresh neuroblastoma cells in fresh cell culture medium to start the next round of tumor cocultures. At the conclusion of the fourth cycle, NKT cells were counted, and the coculture was analyzed by flow cytometry.

Multiplex cytokine quantification assay and ELISA

Culture supernatants of NKTs alone or after 48 hours of coculture with CHLA-255 were collected to measure IL15 release using the Human IL15 ELISA Kit (R&D Systems). Supernatants from *in vitro* cultures of NKTs with and without CHLA-255 cells were collected after 24 hours and analyzed for expression of IFNγ, IL4, GM-CSF, TNFα, and IL10 using the MILLIPLEX MAP Human Cytokine/Chemokine Immunoassay kit (Millipore) for Luminex analysis. Mouse IL6 levels in the plasma were determined using the mouse IL6 ELISA kit (R&D Systems).

***In vivo* studies**

NSG mice were obtained from The Jackson Laboratory and maintained at the BCM animal care facility. For *in vivo* persistence experiments, mice were injected intravenously (i.v.) with 1×10^6 CHLA-255 cells. NKTs were cotransduced with a GD2.CAR and firefly luciferase using retroviral constructs. Seven days after tumor engraftment, approximately 5×10^6 CAR-NKTs or control NKTs were injected i.v. into tumor-bearing mice and monitored using bioluminescent imaging every 2 days (Small Animal Imaging core facility, Texas Children's Hospital). At the time of euthanasia, blood, spleen, liver, lung, and bone marrow were collected, and cells were processed for flow cytometry analysis. For *in vivo* therapeutic experiments, mice were injected i.v. with 1×10^6 firefly luciferase-labeled CHLA-255, CHLA-136, or 2×10^6 LA-N-1 neuroblastoma cells. On day 7, mice were treated with 5×10^6 CAR-NKTs followed by intraperitoneal (i.p.) injection of IL2 (2000 U/mouse) every other day for 2 weeks. Tumor growth was assessed twice weekly by bioluminescent imaging. Animal experiments were performed according to IACUC-approved protocols (BCM IACUC protocol AN-5194).

Immunofluorescent microscopy analyses

Livers of nontransduced, IL15, GD2.28z, and GD2.28z.15 mice were cryosectioned, fixed, and immunostained with anti-human Vα24Jα18 TCR Biotin (clone 6B11, eBioscience), streptavidin Alexa Fluor 488 conjugate (Thermo Fisher), and anti-tyrosine hydroxylase Alexa Fluor 555 conjugate (clone LNC1, Millipore). Slides were costained with ProLong Gold Antifade Reagent with DAPI (Thermo Fisher) and images were obtained using an LSM 780 Confocal Microscope (Zeiss).

Statistical analysis

For *in vitro* and *in vivo* experiments, two-sided unpaired or paired Student *t* tests were used to evaluate differences in continuous variables between two groups. One-way ANOVA with posttest Bonferroni correction was used for continuous variables among more than 2 groups, and two-way ANOVA was used when 2 independent variables were considered. Survival was analyzed using the Kaplan–Meier method and the log-rank (Mantel–Cox) test to compare 2 groups. Statistics were computed using GraphPad Prism 7.0 (GraphPad Software). Differences were considered significant when the *P* value was less than 0.05.

Results

Generation and functional testing of NKTs expressing CAR constructs with or without IL15

We generated retroviral constructs incorporating an optimized 14G2a scFv, human CD8α-derived hinge and transmembrane domains, a human CD28 (GD2.28z) or 4-1BB (GD2.BBz) costimulatory endodomain, and a human CD3ζ signaling domain (ref. 19 and Supplementary Fig. S1A). The cDNA sequence encoding human IL15 was added to GD2.28z (GD2.28z.15) or GD2.BBz (GD2.BBz.15) CAR constructs following a self-cleaving viral 2A peptide sequence, allowing production of separate peptide fragments from a single mRNA. Primary human NKTs were expanded *ex vivo* following the procedure outlined in Supplementary Fig. S1B and stably transduced with each of the 4 constructs. CAR expression in NKTs was similar for all constructs as assessed 3 days after transduction (Fig. 1A). NKTs expressing GD2.28z.15 and GD2.BBz.15 secreted IL15 following a 48-hour culture without or with GD2-positive CHLA-255 neuroblastoma cells, with higher levels observed in the latter condition following NKT activation by CAR engagement (Supplementary Fig. S1C and S1D).

GD2.28z and GD2.28z.15 NKTs had on average 1.25- and 1.14-fold lower expansion rates than nontransduced (NT) NKTs, respectively, at day 10 after secondary stimulation (Fig. 1B). GD2.BBz and GD2.BBz.15 NKT expansion rates dropped to 2.71- and 1.67-fold lower on average than those of NT NKTs, respectively, and were also significantly lower than those of their respective CD28-based counterparts ($P < 0.0001$). When only CAR-positive cells were considered, IL15 expression increased absolute numbers of NKTs expressing both CD28- and 4-1BB–based constructs (Fig. 1C). Flow cytometry analysis of CAR-NKTs 5 days after transduction revealed a significantly higher proportion of early apoptotic cells (annexin-V–positive/7-AAD–negative) in GD2.BBz NKTs versus GD2.28z NKTs (53.4% ± 8.8% vs. 25.9% ± 7.45%, $P < 0.01$) and in GD2.BBz.15 NKTs versus GD2.28z.15 NKTs (28.7% ± 8.14% vs. 8.2% ± 2.88%, $P < 0.05$; Fig. 1D and E). Furthermore, 4-1BB-CAR-NKTs expressed markedly elevated levels of TNF-related apoptosis-inducing ligand (TRAIL; Fig. 1F) and FAS (Supplementary Fig. S2A) compared with CD28-CAR-NKTs. We also found that all CAR-NKT groups expressed death receptor TRAIL-R1 (DR4) and to a lesser extent FASL (Supplementary Fig. S2A and S2B), which together with TRAIL and FAS, respectively, could lead to self-initiated death receptor signaling in these cells. Indeed, we found higher levels of death receptor–dependent caspase-8 activity in 4-1BB-CAR-NKTs than CD28-CAR-NKTs (Fig. 1G). Thus, the 4-1BB costimulatory endodomain induces AICD, leading to loss of CAR-NKTs during *ex vivo* expansion. Instead, NKTs transduced with CD28-containing GD2.CAR constructs—particularly with IL15—undergo relatively low levels of AICD and are capable of extensive numeric expansion, making them a superior option for generating clinical-scale CAR-NKT cell products. Therefore, we selected the GD2.28z and GD2.28z.15 constructs for further preclinical evaluation.

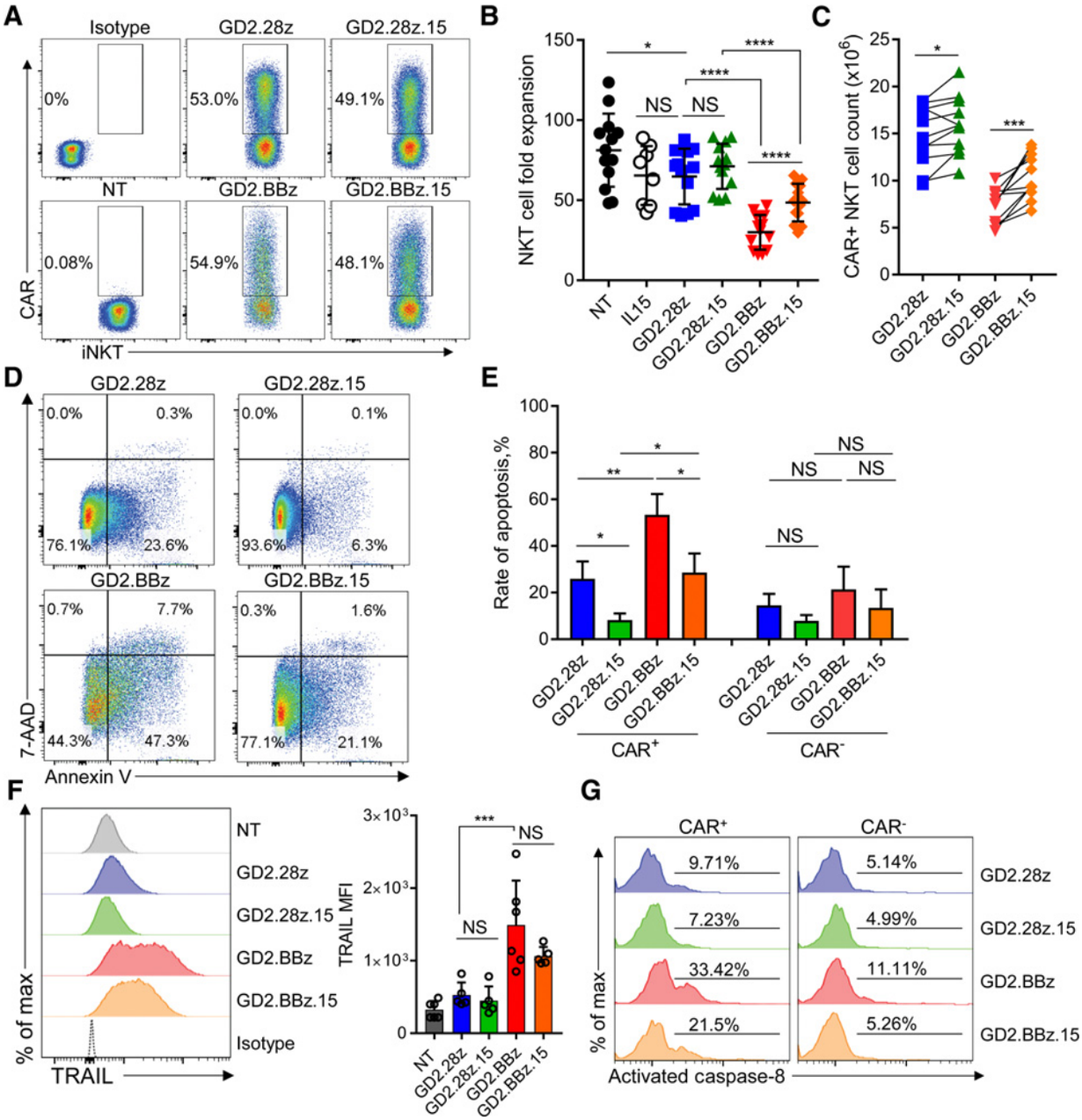

Figure 1.

GD2.CAR constructs containing CD28 costimulatory endodomain enable superior *ex vivo* expansion of CAR-NKTs. **A,** Following a 10-day primary stimulation with α-GalCer–pulsed autologous PBMCs, NKTs were restimulated and transduced 2 days later with the indicated CAR constructs or no construct (NT: nontransduced). Representative flow cytometry analysis of indicated GD2.CAR construct expression 3 days after transduction by gating on $1A7^+$ (14G2a anti-idiotype)/ $V\alpha24\text{-}J\alpha18^+$ NKT cells ($n = 13$). **B,** Quantification of total NKT cell fold expansion, mean ± SD following 10 days of secondary expansion ($n = 13$). NKT cell number was determined using the Cellometer Auto Cell Viability Counter with AOPI staining. *, $P < 0.05$; ****, $P < 0.0001$; NS, not significant; one-way ANOVA. **C,** Quantification of CAR^+ NKT cell expansion calculated following 10 days of secondary expansion. *, $P < 0.05$; ***, $P < 0.001$, Student paired *t* test. **D,** NKTs transduced with the indicated GD2.CAR constructs were stained with annexin V and 7-AAD 5 days after transduction. Shown are representative results from one of 4 donors. **E,** Quantification of annexin V^+/7-AAD- NKTs ± SD in both CAR^+ gated and CAR^- gated populations for indicated GD2.CAR NKT groups ($n = 4$). *, $P < 0.05$; **, $P < 0.01$; NS, not significant; one-way ANOVA. **F,** TRAIL expression in CAR^+ gated populations for the indicated GD2.CAR NKTs 7 days after transduction. Shown are TRAIL median fluorescence intensity (MFI) results from a representative donor and mean ± SD of TRAIL expression MFI from 6 donors. ***, $P < 0.001$; NS, not significant; one-way ANOVA. **G,** Levels of activated caspase 8 were evaluated in the indicated CAR^+ and CAR^- NKT populations using FAM-LETD-FMK labeling 7 days after transduction. Shown are representative results from one of 3 donors.

Coexpression of IL15 enhances survival and reduces exhaustion-associated phenotype in GD2.CAR NKTs

Coexpression of IL15 with a CAR construct should provide a survival advantage for effector cells in the immunosuppressive tumor microenvironment. To determine whether transgenic IL15 coexpressed with the GD2.CAR mediates this intended effect, we cultured GD2.28z and GD2.28z.15 NKTs in cytokine-deprived serum-free medium and evaluated key molecules of the IL15-mediated prosurvival signaling pathway. We found that GD2.28z.15, but not GD2.28z, NKTs robustly phosphorylated Stat5 (Fig. 2A) and upregulated expression of Bcl-2 family members Bcl-2 (Fig. 2B) and Bcl-xL (Fig. 2C), indicating that transgenic IL15 recapitulates the prosurvival functionality of the natural cytokine.

Next, we examined expression trends for major human NKT functional markers CD4 and CD62L in GD2.28z and GD2.28z.15 NKTs at the end of *in vitro* expansion. We confirmed previously reported interindividual variability in CD4 expression across all donors tested (28). NKTs from donors with high frequency of $CD4^+$ cells (80%–100%) retained a high proportion of $CD4^+$ NKTs after CAR transduction (Fig. 2D). In contrast, NKTs from donors with low to intermediate levels of CD4 expression (20%–50%) either decreased or increased the proportion of $CD4^+$ cells after CAR transduction. We detected a consistent decrease in the proportion of $CD62L^+$ NKTs in CAR-transduced versus NT cells, which is likely due to residual tonic signaling induced by GD2.CAR, a common phenomenon in the currently used CARs (29). However, GD2.28z.15 NKTs retained a significantly higher proportion of $CD62L^+$ cells compared with GD2.28z NKTs in 9 of 11 donors (Fig. 2E). Evaluation of exhaustion marker levels revealed that CAR expression led to significant upregulation of PD-1, TIM-3, and LAG-3 in NKTs (Fig. 2F). However, GD2.28z.15 NKTs expressed significantly lower levels of PD-1, TIM-3, LAG-3, and TIGIT (Fig. 2F) and were characterized by significantly fewer cells positive for three of the exhaustion-associated markers than GD2.28z NKTs (Fig. 2G). There was no significant difference in the level of CAR expression observed between the GD2.28z and GD2.28z.15 NKTs ($P > 0.05$, paired t test, $n = 6$). The addition of soluble IL15 to NKT cell culture medium for 7 days after TCR stimulation similarly reduced PD-1 expression in nontransduced and GD2.28z NKTs (Supplementary Fig. S3E). Therefore, coexpression of IL15 with the GD2.CAR enhances NKT survival and alleviates the exhaustion phenotype.

Coexpression of IL15 enhances *in vitro* functional fitness of GD2.CAR NKTs

To determine the efficacy of CAR-mediated killing by NKT cells, we cocultured GD2.CAR NKTs with firefly luciferase (Ffluc)-expressing CD1d-negative and GD2-high (CHLA-255 and LA-N-1), GD2-medium (CHLA-136), or GD2-negative (LA-N-6) neuroblastoma cells (Fig. 3A) for 4 hours. NKTs expressing either GD2.28z or GD2.28z.15 did not kill GD2-negative LA-N-6 cells but mediated equally potent short-term cytotoxicity against GD2-high neuroblastoma cell lines (Fig. 3B). GD2-medium CHLA-136 cells were killed less effectively than GD2-high lines in 4 hours but were eliminated by either GD2.28z or GD2.28z.15 NKTs within 24 hours (Fig. 3C). Although parental NKTs did not kill CD1d-negative neuroblastoma cells, GD2.CAR NKTs retained their native CD1d-restricted reactivity, as they killed α-galactosylceramide-pulsed M2-polarized macrophages (GD2-negative/CD1d-positive) as effectively as parental NKTs (Fig. 3D). Next, we examined changes in GD2.CAR NKT numbers and phenotype after challenge with neuroblastoma cells. Seven days after adding any of 3 neuroblastoma cell lines, GD2.28z.15 mediated expansion/survival of significantly higher numbers of NKTs compared with GD2.28z. However, challenge with CHLA-136 cells resulted in fewer GD2.CAR NKTs compared with CHLA-255 or LA-N-1 cells (Fig. 3E).

To directly test functional fitness, we cocultured GD2.CAR NKTs with GFP-transduced neuroblastoma cells for 5 days, then added equal numbers of the effector cells to fresh tumor cells for another 5 days and repeated such settings in 4 rounds. At the end of each round, viable NKT and neuroblastoma cells were analyzed by flow cytometry (Supplementary Fig. S3A and S3B). We found that GD2.28z.15 mediated greater NKT cell numeric expansion after each round compared with GD2.28z (Fig. 3F). Although NKTs expressing either CAR construct effectively eliminated neuroblastoma cells in the first 3 rounds, GD2.28z.15 was more effective in controlling tumor cell numbers compared with GD2.28z at the end of the fourth round (Fig. 3G). Flow cytometry analysis of NKTs after the fourth round revealed higher levels of PD-1 and TIGIT expression in NKTs transduced with GD2.28z compared with GD2.28z.15 (Supplementary Fig. S3C), suggesting that the presence of IL15 in the CAR construct attenuates NKT cell exhaustion. Similar results were obtained in a repeat challenge experiment using an IncuCyte instrument, which allows continuous measurement of viable tumor cells in coculture with CAR-NKTs (Supplementary Fig. S3D).

To further evaluate the functional potential of GD2.CAR NKTs, we determined their cytokine production profiles in response to stimulation with CHLA-255 neuroblastoma cells. GD2.28z and GD2.28z.15 NKTs both produced high levels of T_H1 cytokine interferon-γ (IFNγ) in the presence CHLA-255 cells, with levels approximately 2-fold higher in GD2.28z.15 NKTs (Fig. 3H). Both groups produced similar levels of T_H2 cytokine IL4, resulting in an overall higher IFNγ-to-IL-4 ratio in GD2.CAR NKTs with IL15 (Fig. 3I). Similar trends were observed with T_H1 cytokines GM-CSF and TNFα, while IL10 was not detected from either GD2.CAR NKT group (Supplementary Fig. S4).

GD2.28z.15 construct supports superior NKT cell *in vivo* persistence

Long-term persistence of CAR-effector cells is critical to the success of adoptive cell therapies (30–33). We examined the *in vivo* persistence of GD2.28z and GD2.28z.15 NKTs cotransduced with high-intensity Ffluc cDNA following transfer into NSG mice with 7-day established neuroblastoma xenografts (Fig. 4A). Mice injected with Ffluc-only and IL15/Ffluc NKTs served as control groups. Transgenic expression of IL15 on its own improved NKT persistence compared with NT/Ffluc NKTs while GD2.28z only marginally boosted persistence above NT/Ffluc control (Fig. 4B and C). Importantly, addition of IL15 to the GD2.28z construct significantly enhanced the ability of infused NKTs to expand and persist beyond levels seen in GD2.28z or IL15 NKTs. We checked the bone marrow, the primary site of neuroblastoma metastases in humans and our mouse model, for the presence of tumor and NKTs 20 days after NKT cell transfer. Both IL15/Ffluc and GD2.28z.15 NKT cells were present at approximately 6 times higher frequency in the bone marrow than NT/Ffluc NKTs, while GD2.28z NKT frequency did not exceed that of control NKTs (Fig. 4D). Accordingly, mice treated with

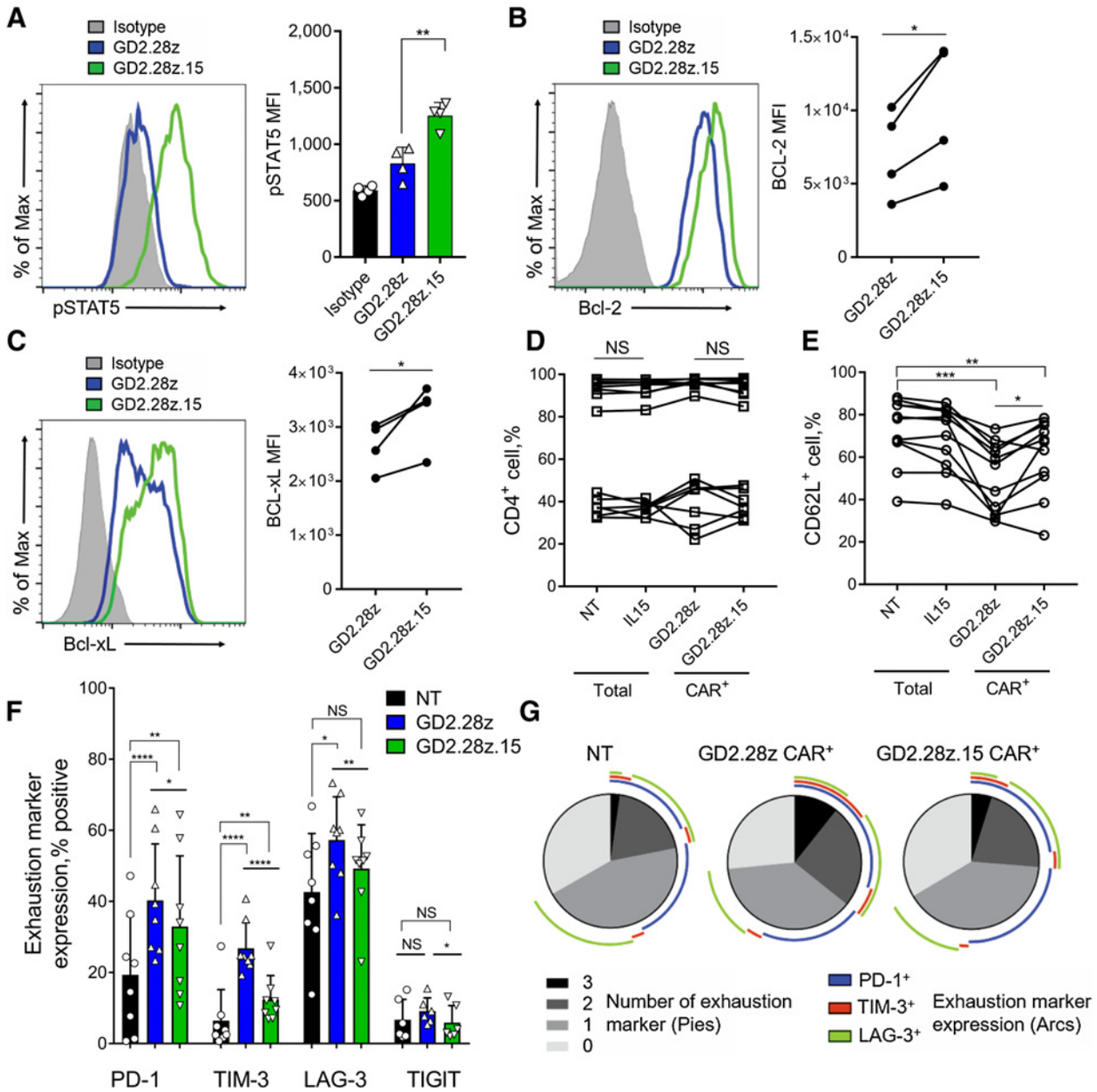

Figure 2.

Coexpression of IL15 enhances survival and reduces exhaustion-associated phenotype in GD2.CAR NKTs. **A,** Expression of phosphorylated STAT5 (pSTAT5) was evaluated in NKTs expressing the GD2.28z or GD2.28z.15 CAR 7 days after transduction following 12 hours of culture in serum- and cytokine-starved conditions. Shown is a representative histogram from one of 4 donors (left) and mean ± SD of MFI for all donors ($n = 4$). **, $P < 0.01$, one-way ANOVA. **B,** Expression of intracellular Bcl-2 was evaluated in NKTs expressing the GD2.28z or GD2.28z.15 CAR 7 days after transduction following 12 hours of culture in serum- and cytokine-starved conditions. Shown is a representative histogram from 1 of 4 donors (left) and Bcl-2 expression MFI for each individual donor expressing the GD2.28z versus the GD2.28z.15 CAR ($n = 4$). *, $P < 0.05$, Student paired *t* test. **C,** Expression of intracellular Bcl-xL was evaluated in NKTs expressing the GD2.28z or GD2.28z.15 CAR 7 days after transduction following 12 hours of culture in serum- and cytokine-starved conditions. Shown is a representative histogram from 1 of 4 donors (left) and Bcl-xL expression MFI for each individual donor expressing the GD2.28z versus the GD2.28z.15 CAR ($n = 4$). *, $P < 0.05$, Student paired *t* test. **D,** Following 21-day *in vitro* expansion, NKTs from 14 individual donors transduced with the indicated constructs or nontransduced (NT) NKTs were evaluated for CD4 expression and (**E**) 11 of them were also examined for CD62L expression by flow cytometry. NS, not significant; *, $P < 0.05$; **, $P < 0.01$; ***, $P < 0.001$, Student paired *t* test. **F,** NKTs transduced with the GD2.28z or GD2.28z.15 CAR or NT were evaluated for expression of the indicated exhaustion markers 7 days after transduction ($n = 8$). *, $P < 0.05$; **, $P < 0.01$; ****, $P < 0.0001$; NS, not significant; one-way ANOVA. **G,** SPICE analysis of exhaustion marker expression from 3 of the donors shown in **F**. Pie charts reflect proportions of indicated NKT groups expressing indicated numbers (0–3) of exhaustion markers. Colored arcs indicate the specific combinations of exhaustion markers expressed.

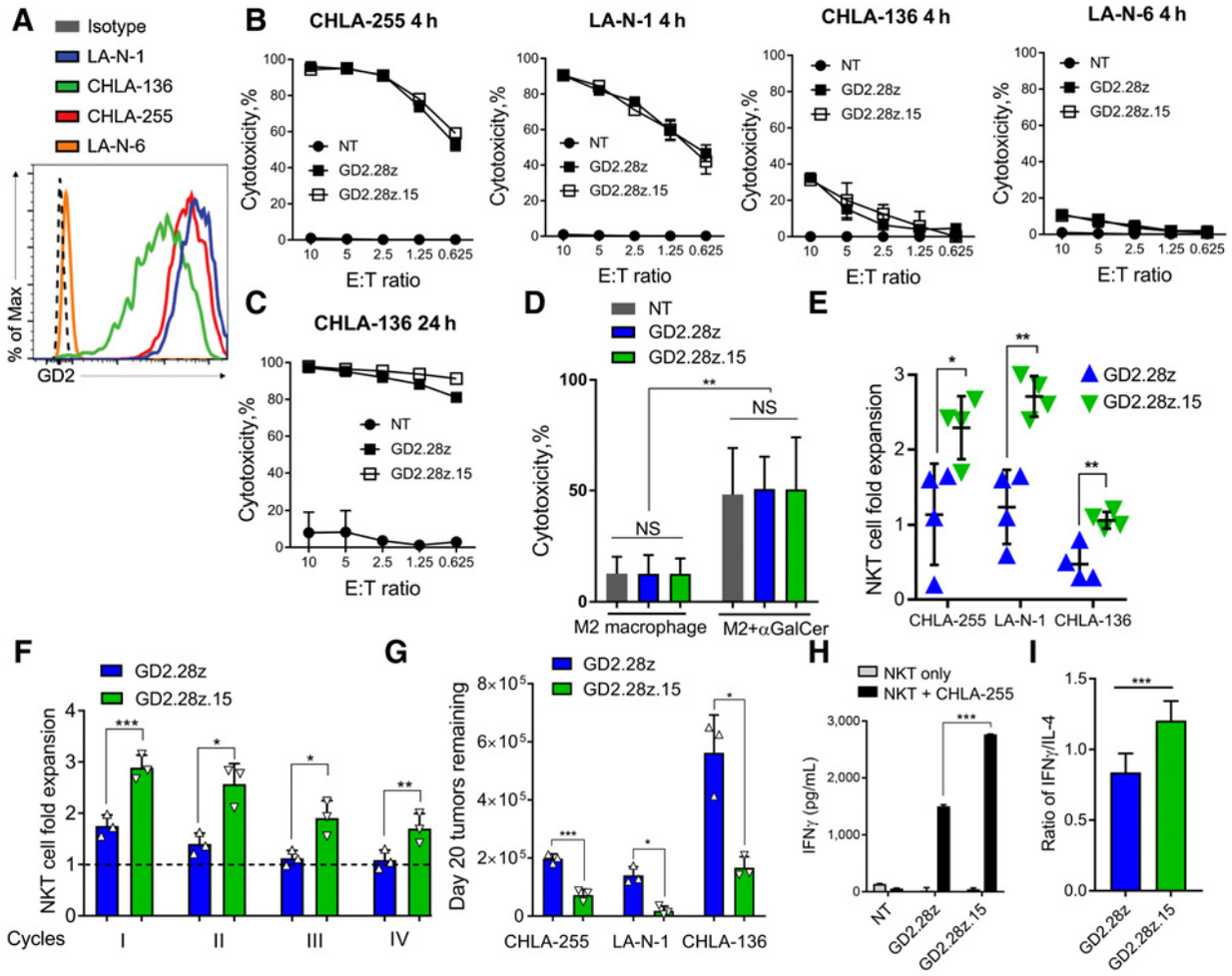

Figure 3.

Coexpression of IL15 enhances the *in vitro* functional fitness of GD2.CAR NKTs. **A,** Flow cytometry analysis of GD2 expression in the indicated neuroblastoma cell lines. **B,** The indicated luciferase-transduced neuroblastoma cell lines were cocultured with GD2.CAR NKTs for 4 or (**C**) 24 hours. Cytotoxicity was calculated by measuring luminescence intensity of lysed target cells with a plate reader. Shown are results from a representative of 4 experiments (each with a separate NKT donor) with 3 technical replicates. **D,** GD2.CAR NKTs were cocultured with calcein-AM–labeled M2-polarized macrophages with or without α-GalCer for 4 hours. Cytotoxicity was assessed by flow cytometry. Shown are mean ± SD from 4 donors. **, $P < 0.01$; NS, not significant; two-way ANOVA. **E,** NKT cell fold expansion measured after 1:1 coculture with neuroblastoma cells for 7 days with 50 U/mL IL2. NKT cell number was determined using the cell counter and flow cytometry. Shown are mean ± SD from 4 donors. *, $P < 0.05$; **, $P < 0.01$, Student unpaired *t* test. **F,** Neuroblastoma cells expressing GFP were plated at a 1:1 effector-to-target (E:T) ratio with GD2.CAR NKTs every 5 days for 4 cycles. NKT cells were harvested from the previous coculture and then replated in new culture medium with fresh tumor cells at the same 1:1 E:T ratio. At each cycle, cells were counted and analyzed by flow cytometry. Shown are results of a representative cell line, CHLA-255, from one of 2 independent experiments performed with 3 NKT donors per experiment. *, $P < 0.05$; **, $P < 0.01$; ***, $P < 0.001$, Student paired *t* test. **G,** Tumor cells remaining after cycle 4 following the experiment described in **F**. *, $P < 0.05$; ***, $P < 0.001$, Student paired *t* test. **H,** GD2.CAR NKTs were stimulated with CHLA-255 cells or left unstimulated and supernatants were collected at 24 hours. IFNγ concentrations were measured by Luminex assay. Shown are mean ± SD from a representative of 3 experiments with 3 technical replicates. ***, $P < 0.001$, two-way ANOVA. **I,** Ratio of IFNγ-to-IL4 production by GD2.CAR NKTs following 24-hour coculture with CHLA-255 cells. Shown are mean ± SD for 3 donors with 3 replicates each. ***, $P < 0.001$, Student unpaired *t* test.

GD2.28z.15 NKTs had significantly fewer neuroblastoma cells in the bone marrow than mice treated with GD2.28z NKTs (Fig. 4E).

GD2.28z.15 construct mediates effective infiltration of NKTs into solid tumor tissues

To control tumor growth, therapeutic effector cells must effectively traffic to the tumor site. Using tumor tissues from neuroblastoma nodules in the livers of NSG mice (Fig. 5A), we performed confocal microscopy to evaluate the ability of GD2.CAR NKTs to infiltrate the tumor 13 days after treatment. Consistent with previous observations (12, 15), we found that transgenic expression of either IL15 alone or a GD2.CAR significantly increased the frequency of NKTs in the tumor tissue as compared with control NKTs (Fig. 5B and C). GD2.28z.15 NKTs were present at significantly higher numbers within neuroblastoma nodules than both GD2.28z NKTs and IL15-only NKTs (Fig. 5B and C). In addition to the tumor, GD2.28z and GD2.28z.15 CAR-NKTs were detected in the spleen, liver, bone marrow, and lung (Fig. 5D). Within these tissues, GD2.28z.15 NKTs were predominantly $CD4^-$ compared with GD2.28z NKTs (Fig. 5E), indicating

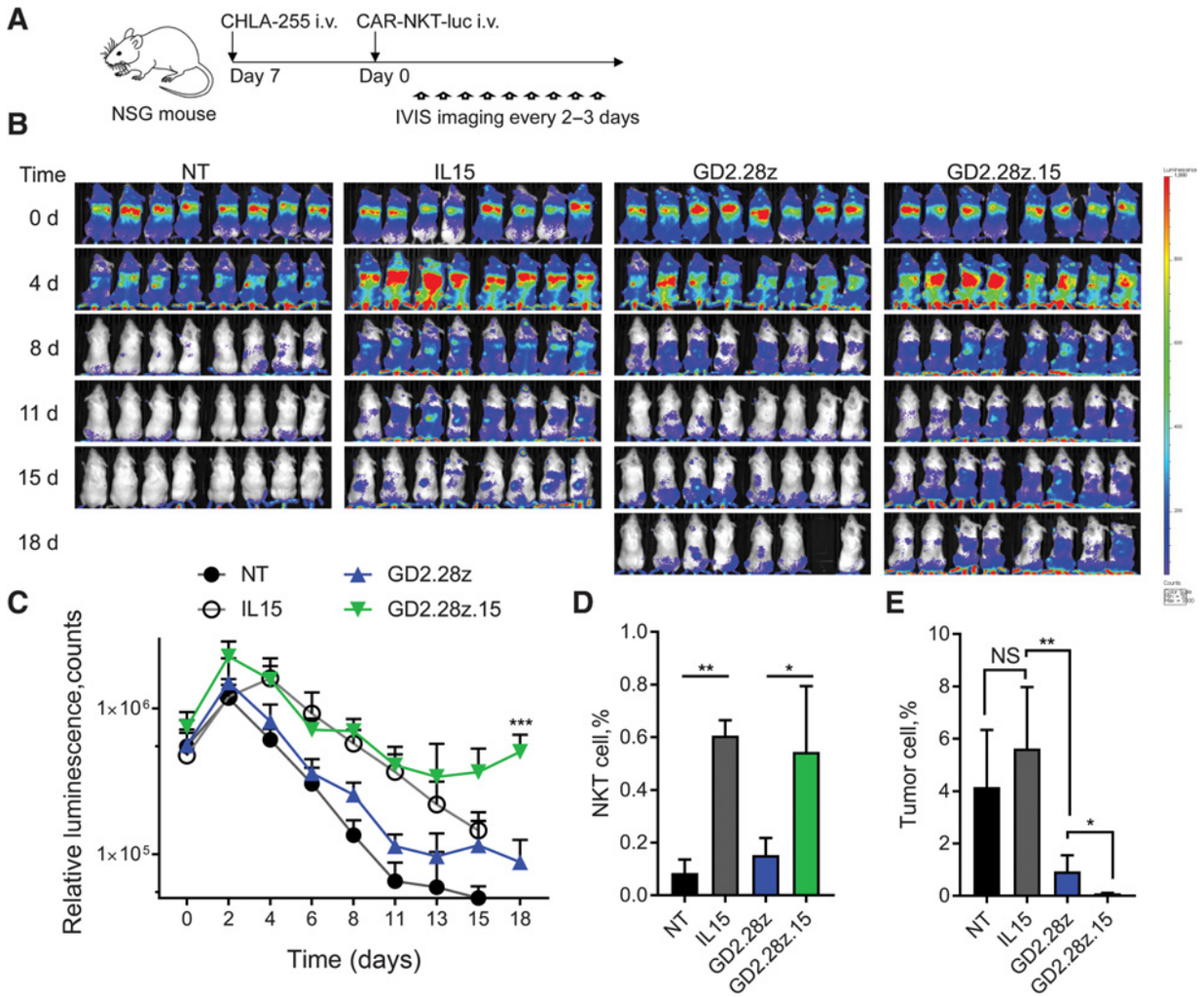

Figure 4.

The GD2.28z.15 construct supports superior NKT cell *in vivo* persistence. **A,** Overview of *in vivo* NKT persistence experiments. NSG mice were injected intravenously with CHLA-255 neuroblastoma cells followed 7 days later by luciferase-labeled CAR.GD2 or control NKTs. NKTs were tracked by bioluminescence imaging every 2 to 3 days. **B,** Bioluminescent monitoring of NT, IL15, GD2.28z, and GD2.28z.15 NKTs injected into groups of mice ($n = 8$/group) carrying CHLA-255 xenografts. Shown are representative results from one of 3 experiments (each with a separate NKT donor). **C,** Quantification of bioluminescence images in **B**. ***, $P < 0.001$, GD2.28z versus GD2.28z.15, Student unpaired *t* test. **D,** Quantification of NKT cells (human $CD45^+/NKT^+$) in total bone marrow cells at day 20 as determined by flow cytometry. *, $P < 0.05$; **, $P < 0.01$, one-way ANOVA. **E,** Quantification of neuroblastoma tumor cells (human $CD56^+/GD2^+$) in total bone marrow cells at day 20 as determined by flow cytometry. Five mice in both NT and IL15 groups were granted exceptions to delay euthanasia until day 20, but could not be imaged on day 18. *, $P < 0.05$; **, $P < 0.01$; NS, not significant; Student unpaired *t* test.

that local IL15 production preferentially benefits survival and/or expansion of $CD4^-$ over $CD4^+$ NKTs. CD62L expression was generally low in GD2.CAR NKTs infiltrating the tissues regardless of transgenic IL15 (Fig. 5F). At the later time point (8 weeks) after infusion, CAR-NKTs could still be found in bone marrow at the frequencies of 6.26% ± 1.006% and 0.026% ± 0.003% for GD2.28z.15 and GD2.28z, respectively (Fig. 5G; $P < 0.001$). Again, these long-term persisting GD2.28z.15 NKTs were preferentially $CD4^-$ cells in 3 experiments from NKT cell donors with 20%–50% $CD4^+$ NKT frequency in peripheral blood (Fig. 5H). However, GD2.28z.15 NKTs from one donor with a high proportion of the $CD4^+$ subset at baseline still exhibited increased persistence in bone marrow while retaining CD4 expression (Supplementary Fig. S5A and S5B). Therefore, GD2.28z.15 NKTs effectively home to and persist in tumor tissues, in particular due to increased survival and/or expansion of the $CD4^-$ subset with a possible exception for donors with a high proportion of $CD4^+$ NKTs.

GD2.28z.15 construct enables superior therapeutic activity of GD2.CAR NKTs in mice without significant toxicity

We next evaluated the ability of GD2.CAR NKTs to control tumor growth in 3 xenogeneic neuroblastoma models. NSG mice were intravenously injected with CHLA-255, LA-N-1, or CHLA-136 neuroblastoma cells stably expressing Ffluc, and 7 days later they received 5×10^6 of either GD2.28z or GD2.28z.15 NKTs intravenously (Fig. 6A). Mice treated with NT or IL15-transduced NKTs were used as control groups. We found that GD2.28z.15

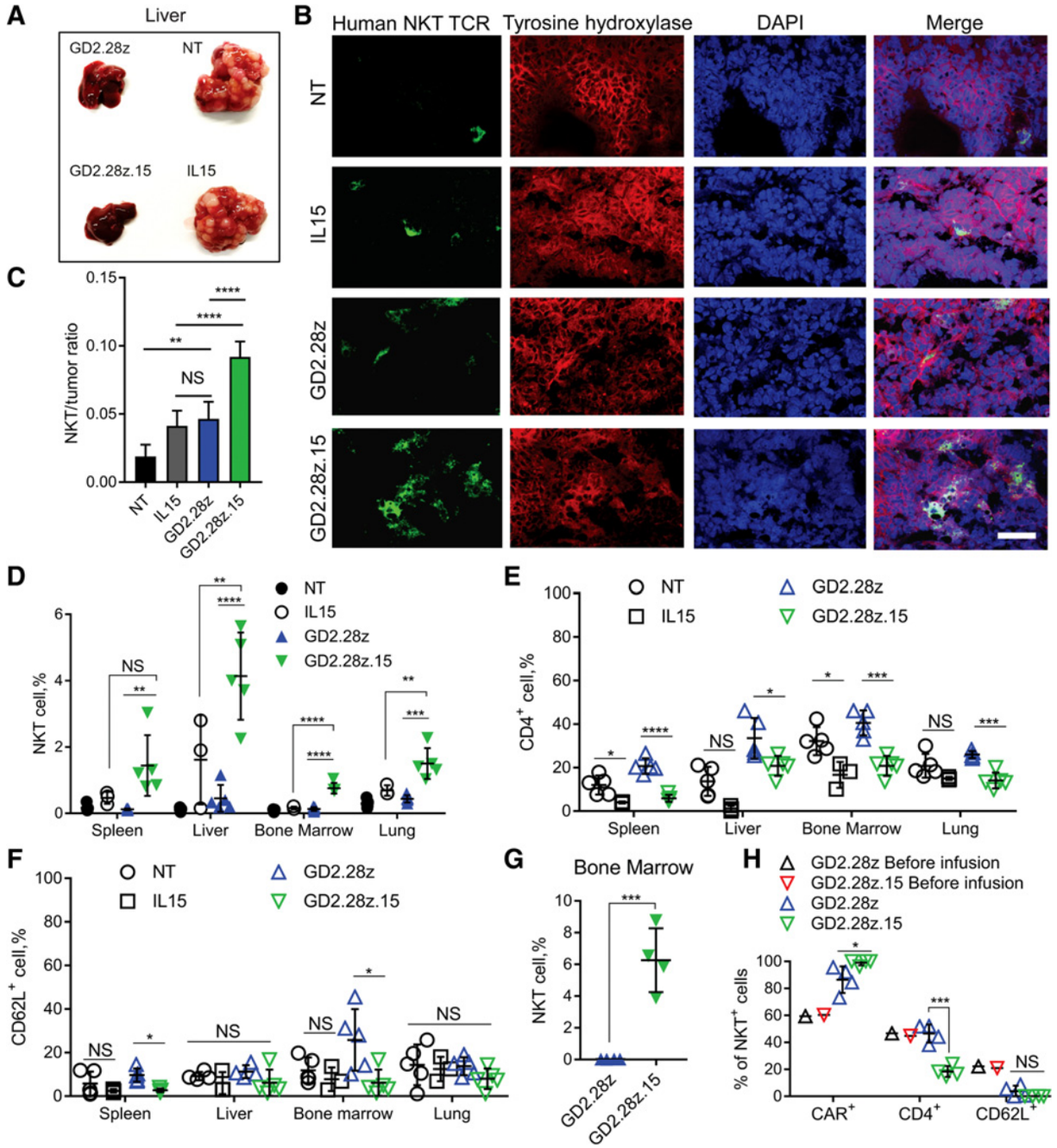

Figure 5.

GD2.28z.15 mediates effective infiltration of NKTs into solid tumor tissues and expansion of CD4-negative NKTs. **A,** CHLA-255–bearing NSG mice were injected with luciferase-labeled GD2.CAR or control NKTs in a similar experimental setup as shown in Fig. 4A. Thirteen days after injection of NKTs, resected livers were photographed. Shown are representative images from 5 mice per group, 1 of 3 experiments. **B,** Liver metastases from **A** were fixed and processed for cryosectioning. Sections were probed with antibodies against the Vα24-Jα18 NKT TCR, neuroblastoma tumor marker tyrosine hydroxylase, and DAPI. Images were visualized and quantified by confocal microscopy. **C,** Absolute numbers of NKT cells and tumor cells were counted in 10 fields per mouse using images in **B**, 5 mice per group. **, $P < 0.01$; ****, $P < 0.0001$; NS, not significant; one-way ANOVA. **D,** Quantification of human NKT cells (human $CD45^+/NKT^+$) in total cell populations collected from indicated organs ($n = 5$), 1 of 3 experiments. **, $P < 0.01$; ***, $P < 0.001$; ****, $P < 0.0001$; NS, not significant; one-way ANOVA. **E,** Quantification of $CD4^+$ NKT cells in total cell populations collected from indicated organs ($n = 5$). *, $P < 0.05$; ***, $P < 0.001$; ****, $P < 0.0001$; NS, not significant; one-way ANOVA. **F,** Quantification of $CD62L^+$ NKT cells in total cell populations collected from indicated organs ($n = 5$). *, $P < 0.05$; NS, not significant; one-way ANOVA. **G,** At week 8 after injection, human NKT cells were quantified in total cell populations collected from bone marrow ($n = 4$). ***, $P < 0.001$, Student unpaired *t* test. **H,** Quantification of CAR^+, $CD4^+$, or $CD62L^+$ subsets of NKT cells in bone marrow as in **G** ($n = 4$). Data from a representative of 3 independent experiments. *, $P < 0.05$; ***, $P < 0.001$; NS, not significant; Student unpaired *t* test.

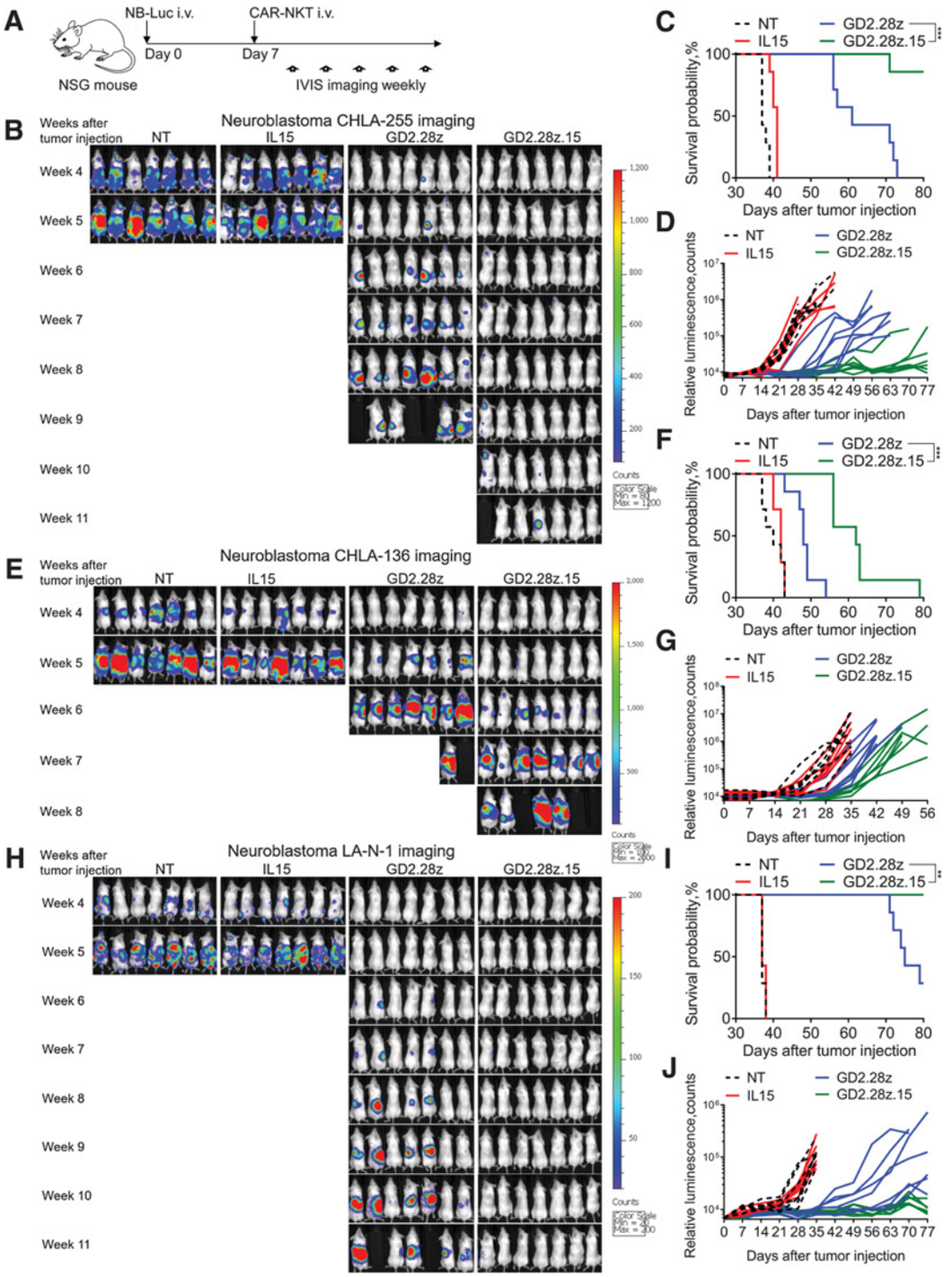

Figure 6.

GD2.28z.15 enables superior *in vivo* therapeutic activity of GD2.CAR NKTs without causing significant toxicity. **A,** Schematic representation of *in vivo* tumor challenge experiments. NSG mice were injected intravenously with luciferase-labeled neuroblastoma cell lines followed 7 days later by CAR.GD2 NKTs. Tumor growth was assessed weekly by bioluminescence imaging. **B,** Weekly bioluminescent monitoring of CHLA-255 tumor growth in mice ($n = 7$/group). **C,** Kaplan–Meier curve generated from survival of animals in **B**. ***, $P < 0.001$ log-rank (Mantel–Cox). **D,** Quantification of bioluminescence in **B**. **E,** Weekly bioluminescent monitoring of CHLA-136 tumor growth. **F,** Kaplan–Meier curve generated from survival of animals in **E**. ***, $P < 0.001$ log-rank (Mantel–Cox). **G,** Quantification of bioluminescence in **E**. **H,** Weekly bioluminescent monitoring of LA-N-1 tumor growth. **I,** Kaplan–Meier curve generated from survival of animals in **H**. **, $P < 0.01$ log-rank (Mantel–Cox). **J,** Quantification of bioluminescence in **H**. Shown are representative results from 1 of 4 independent experiments with the CHLA-255 model and one experiment each for the CHLA-136 and LA-N-1 models.

NKTs controlled tumor growth significantly longer than GD2.28z NKTs in all three neuroblastoma models ($P < 0.001$; Fig. 6B–J). The GD2.28z.15 NKT cell therapy was particularly effective against xenografts of 2 neuroblastoma cell lines with high-level GD2 expression, mediating prolonged survival of the majority of mice without evidence of disease up to three months postinfusion when animals were sacrificed. We also treated CHLA-255 tumor–bearing mice with a lower (2×10^6) or a higher (10^7) dose of CAR-NKTs. Supplementary Fig. S6 demonstrates that NKTs expressing the IL15-containing CAR retain superior antitumor activity at a low and a high dose. Moreover, only GD2.28z.15 NKT therapy mediated long-term disease-free survival in the majority of mice at the high dose. Thus, consistent with its ability to mediate the longest duration of *in vivo* persistence and most effective tumor infiltration, GD2.28z.15 also imparted NKTs with superior dose-dependent antitumor activity, especially against tumors with high-level GD2 expression.

We observed mild hunched mouse stature and ruffled fur 12 days after injection of GD2.28z.15 NKTs that completely resolved within 2 to 3 days. At approximately the same time, transient weight loss not exceeding 10% of total body weight also occurred (Supplementary Fig. S7A). Beyond day 14, animals maintained or increased weight. Serum collected on days 12 and 15 was analyzed by ELISA for the presence of human IL15 and murine IL6, the latter of which is produced predominantly by murine macrophages in a manner that parallels the development of cytokine release syndrome in humans (34). Murine IL6 levels were not significantly different between GD2.28z.15 NKT-treated and untreated control mice (Supplementary Fig. S7B), while human IL15 remained undetectable in both groups. Detailed pathologic examination was also performed by an experienced clinical pathologist in mice sacrificed at day 12 or 15 after NKT injection. Lung, heart, liver, spleen, kidney, adrenals, stomach, intestine, pancreas, spine, brain (cerebrum, hippocampus, and cerebellum), skin, bone with bone marrow, and skeletal muscle revealed minimally detectable tumor cells in 2 mice. Additionally, no pathologic abnormalities were detected in any organ or tissue with the exception of the lungs, where mice in both groups exhibited signs of focal minimal-to-mild interstitial inflammation. An additional long-term tissue evaluation performed between 45 and 60 days after injection of GD2.28z.15 NKTs also showed complete absence of toxicity or features of graft-versus-mouse disease (Supplementary Fig. S7C). There was also no tissue toxicity observed including in the brains of mice treated with 10^7 GD2.28z.15 NKTs (Supplementary Fig. S8). Thus, GD2.28z.15 NKTs exert potent anti- neuroblastoma activity without causing significant off-target toxicity in mice.

Discussion

NKTs are a promising cellular platform for CAR-redirected cancer immunotherapy. Our previous studies have demonstrated that NKTs naturally traffic to neuroblastoma in xenograft models in response to tumor-derived chemokines and that their ability to infiltrate tumors is further enhanced by expression of a tumor-specific GD2.CAR (12, 15).

We have also found that NKT cell functionality is inhibited in the hypoxic tumor microenvironment and at least in part rescued by the transgenic expression of IL15 (15). Therefore, we sought to test the hypothesis that coexpression of IL15 with the GD2.CAR would enhance the ability of NKTs to traffic to and attack neuroblastoma tumors. Our results demonstrate that NKTs expressing either GD2.28z or GD2.28z.15, but not GD2.BBz or GD2.BBz.15, CAR constructs can be expanded *ex vivo* to clinical scale and mediate potent CAR-dependent killing of neuroblastoma cells *in vitro*. Compared with GD2.28z, GD2.28z.15 CAR-NKTs demonstrated superior functional fitness, prolonged *in vivo* persistence, and superior tumor control in mice without causing significant toxicity.

When comparing GD2.CAR constructs incorporating the 2 most commonly used costimulatory endodomains, CD28 and 4-1BB, we found that 4-1BB–containing constructs induced higher levels of AICD in NKTs than CD28-containing constructs, regardless of IL15 coexpression. This AICD was associated with increased TRAIL and FAS expression, activation of caspase-8, and induction of apoptosis, resulting in lower overall NKT cell numeric expansion. In line with our findings in NKTs, Mamonkin and colleagues observed that 4-1BB–containing CARs expressed from a retroviral vector with strong LTR promoter activity enhanced AICD levels in transduced T cells (35). Specifically, 4-1BB–mediated TRAF-dependent NFκB activation led to upregulation of death receptors and an increased rate of AICD in CAR T cells.

Although GD2.28z and GD2.28z.15 NKTs were equally effective in short-term cytotoxicity assays against 2 GD2-high (CHLA-255 and LA-N-1) neuroblastoma cell lines, both mediated reduced cytotoxicity against GD2-medium (CHLA-136) neuroblastoma cells. CHLA-255 is an MYCN-nonamplified line while LA-N-1 and CHLA-136 are MYCN-amplified lines, suggesting that the efficacy of CAR.GD2 NKT cell therapy depends on the level of GD2 expression on neuroblastoma cells rather than their MYCN status. GD2.28z.15 NKTs demonstrated significantly more effective tumor control in a repeat challenge assay. This activity was associated with expansion of GD2.28z.15 but not GD2.28z NKTs. We recently showed parallel results with T cells expressing the same 2 constructs; GD2.28z.15 T cells demonstrated superior expansion and antitumor activity after numerous tumor cell exposures compared with GD2.28z T cells (19). Additionally, we have found that expression of IL15-containing CARs is associated with reduced exhaustion marker expression in both T and NKT cells, suggesting that IL15 prevents NKT cell exhaustion in the same manner as it does in T cells.

Coexpression of IL15 with the GD2.CAR enriched for T cells with memory and stem-cell–like phenotypes (19). Although the mechanisms governing memory differentiation of human NKTs remain less explored than those of T cells, we recently demonstrated that $CD62L^+$ central memory–like NKTs can expand in culture and are largely responsible for the *in vivo* persistence and therapeutic potential of CAR-NKTs (16). The addition of IL15 to the CAR increased the frequency of $CD62L^+$ NKTs in 9 of 11 donors examined, suggesting that IL15 protects NKTs from cell death and exhaustion, and may provide a selective advantage for central memory-like NKTs.

After adoptive transfer to tumor-bearing mice, GD2.28z.15 NKTs demonstrated remarkable persistence especially in the bone marrow and liver (primary sites of neuroblastoma metastasis) despite the highly hypoxic microenvironment of neuroblastoma liver metastases that hampers NKT survival and function (15). We previously reported that transgenic IL15 protects NKTs from hypoxia (15), and here we further observed that IL15 promotes survival of CAR-NKTs in neuroblastoma xenografts in the liver. Furthermore, phenotypic analysis of infiltrated CAR-NKTs

revealed enrichment of NKTs expressing low levels of CD62L, suggesting that persistent CAR stimulation promotes effector memory–like differentiation of NKTs as occurs in T cells.

NKTs produce numerous cytokines, which individually may exert either proinflammatory or inhibitory effects. Our *in vitro* testing showed that NKTs coexpressing IL15 and a GD2.CAR predominantly secrete a T_H1-like profile following CAR engagement as evidenced by increased production of IFNγ, GM-CSF, and TNFα as well as an increased IFNγ-to-IL4 ratio. This observation is consistent with our previous findings showing higher expression of the IL2Rβ/IL-15Rβ subunit (CD122) in $CD4^-$ NKTs (21), which produce more T_H1 and less T_H2 cytokines than $CD4^+$ NKTs (28). Moreover, in murine models, $CD4^-$ NKTs have been reported to have better antitumor functionality *in vitro* and *in vivo* compared with their $CD4^+$ counterparts (36). Despite increased sensitivity of $CD4^-$ NKTs to IL15, we did not observe consistent changes in $CD4^+/CD4^-$ proportion during *in vitro* expansion of GD2.28z and GD2.28z.15 NKTs, likely due to the presence of IL2 in culture medium. In contrast, after adoptive transfer to tumor-bearing mice, GD2.28z.15 NKTs derived from 3 donors with low to intermediate levels of $CD4^+$ cells persisted predominantly as $CD4^-$ cells within the tumor. We did observe, however, that GD2.28z.15 NKTs derived from a donor with a high proportion of $CD4^+$ NKTs retained CD4 expression *in vivo*, a phenomenon that needs to be further explored.

We found that the potent antitumor effect of GD2.28z.15 NKTs occurred without significant toxicity. The pathologic analysis of mouse tissues including brain did not reveal signs of inflammation. In contrast, Richman and colleagues observed lethal CNS toxicity when testing T cells expressing a mutated CAR.GD2 with an increased affinity to GD2 (9), indicating that increasing CAR affinity to GD2 may not be a viable strategy for increasing the therapeutic efficacy of GD2-targetting immunotherapy. Instead, our approach is based on enhancing functionality of the CAR-expressing effector cells that leads to enhanced antitumor activity without evident toxicity to normal tissues. In contrast, systemic administration of IL15 in patients with cancer has been associated with dose-limiting toxicities (37), although IL15/IL15Ra superagonists such as ALT-803 show an increased therapeutic index in the initial clinical testing (38). IL15 remained undetectable in the serum of mice treated with GD2.28z.15 NKTs, indicating that the therapeutic effects of IL15 are likely associated with local release of the cytokine at the tumor site.

Based on results of a randomized phase III clinical trial (39), the FDA approved anti-GD2 monoclonal antibody ch14.18 (dinutuximab) in combination with GM-CSF, IL2, and 13-cis-retinoic acid for maintenance therapy of high-risk neuroblastoma. The antitumor activity of dinutuximab largely depends on antibody-dependent cellular cytotoxicity (ADCC), which is mediated by NK and myeloid cells and augmented by IL2 and GM-CSF, respectively (40, 41). Ch14.18 given as a single agent is ineffective (42). Although the role of individual cytokines in this combination therapy is still under investigation, the current regimen remains toxic and not curative for a third of high-risk patients (43). GD2.28z.15 NKT cell therapy is designed to maximize direct neuroblastoma cell killing without dependence on ADCC or systemic cytokine administration that may lead to a more effective and safe immunotherapy for high-risk and relapsed neuroblastoma.

Disclosure of Potential Conflicts of Interest

A. Heczey reports receiving other commercial research support from Cell Medica. A. N. Courtney holds ownership interest (including patents) in Cell Medica. G. Dotti reports receiving commercial research grants from Cell Medica and is listed as a co-inventor on a patent regarding NKT cells as a cell platform for CAR expression that has been licensed to Cell Medica. L.S. Metelitsa reports receiving commercial research grants from and holds ownership interest (including patents) in Cell Medica. No potential conflicts of interest were disclosed by the other authors.

Authors' Contributions

Conception and design: X. Xu, W. Huang, J. Hicks, H. Ngai, G. Dotti, L.S. Metelitsa

Development of methodology: X. Xu, W. Huang, D. Liu, L. Guo, M. Wood, J. Jin, B. Liu, J. Hicks, G.A. Barragan, B. Savoldo, G. Dotti, L.S. Metelitsa

Acquisition of data (provided animals, acquired and managed patients, provided facilities, etc.): X. Xu, W. Huang, D. Liu, L. Guo, J. Jin, A.N. Courtney, J. Hicks, G.A. Barragan, H. Ngai

Analysis and interpretation of data (e.g., statistical analysis, biostatistics, computational analysis): X. Xu, W. Huang, A. Heczey, L. Guo, J. Jin, A.N. Courtney, J. Hicks, G.A. Barragan, H. Ngai, L.S. Metelitsa

Writing, review, and/or revision of the manuscript: X. Xu, W. Huang, A. Heczey, J. Jin, A.N. Courtney, B. Liu, E.J. Di Pierro, J. Hicks, G.A. Barragan, H. Ngai, G. Dotti, L.S. Metelitsa

Administrative, technical, or material support (i.e., reporting or organizing data, constructing databases): W. Huang, L. Guo, M. Wood, B. Liu, J. Hicks, Y. Chen

Study supervision: X. Xu, W. Huang, G. Dotti, L.S. Metelitsa

Acknowledgments

The authors are grateful for the excellent technical assistance provided by the staff at Flow Cytometry Core Laboratory of the Texas Children's Cancer and Hematology Center, and Small Animal Imaging core facility at Texas Children's Hospital. This work was supported by grants from the NIH (RO1 CA116548 and S10 OD020066 to L.S. Metelitsa), Cell Medica, Ltd (to L.S. Metelitsa), Alex's Lemonade Stand Foundation for Childhood Cancer (to L.S. Metelitsa and A. Heczey), and Cookies for Kids' Cancer Foundation (to L.S. Metelitsa).

The costs of publication of this article were defrayed in part by the payment of page charges. This article must therefore be hereby marked *advertisement* in accordance with 18 U.S.C. Section 1734 solely to indicate this fact.

Received February 1, 2019; revised August 5, 2019; accepted August 27, 2019; published first September 4, 2019.

References

1. Lim WA, June CH. The principles of engineering immune cells to treat cancer. Cell 2017;168:724–40.
2. Brudno JN, Kochenderfer JN. Chimeric antigen receptor T-cell therapies for lymphoma. Nat Rev Clin Oncol 2018;15:31–46.
3. Smith M, Zakrzewski J, James S, Sadelain M. Posttransplant chimeric antigen receptor therapy. Blood 2018;131:1045–52.
4. Dotti G, Gottschalk S, Savoldo B, Brenner MK. Design and development of therapies using chimeric antigen receptor-expressing T cells. Immunol Rev 2014;257:107–26.
5. Watanabe K, Kuramitsu S, Posey AD Jr, June CH. Expanding the therapeutic window for CAR T cell therapy in solid tumors: the knowns and unknowns of CAR T cell biology. Front Immunol 2018;9:2486.
6. Manzo T, Heslop HE, Rooney CM. Antigen-specific T cell therapies for cancer. Hum Mol Genet 2015;24:R67–73.
7. Pule MA, Savoldo B, Myers GD, Rossig C, Russell HV, Dotti G, et al. Virus-specific T cells engineered to coexpress tumor-specific receptors: persistence and antitumor activity in individuals with neuroblastoma. Nat Med 2008;14:1264–70.

8. Louis CU, Savoldo B, Dotti G, Pule M, Yvon E, Myers GD, et al. Antitumor activity and long-term fate of chimeric antigen receptor-positive T cells in patients with neuroblastoma. Blood 2011;118:6050–6.
9. Richman SA, Nunez-Cruz S, Moghimi B, Li LZ, Gershenson ZT, Mourelatos Z, et al. High-affinity GD2-specific CAR T cells induce fatal encephalitis in a preclinical neuroblastoma model. Cancer Immunol Res 2018;6:36–46.
10. Rezvani K, Rouce R, Liu E, Shpall E. Engineering natural killer cells for cancer immunotherapy. Mol Ther 2017;25:1769–81.
11. Harrer DC, Simon B, Fujii SI, Shimizu K, Uslu U, Schuler G, et al. RNA-transfection of gamma/delta T cells with a chimeric antigen receptor or an alpha/beta T-cell receptor: a safer alternative to genetically engineered alpha/beta T cells for the immunotherapy of melanoma. BMC Cancer 2017;17:551.
12. Heczey A, Liu D, Tian G, Courtney AN, Wei J, Marinova E, et al. Invariant NKT cells with chimeric antigen receptor provide a novel platform for safe and effective cancer immunotherapy. Blood 2014;124:2824–33.
13. Metelitsa LS. Anti-tumor potential of type-I NKT cells against CD1d-positive and CD1d-negative tumors in humans. Clin Immunol 2011; 140:119–29.
14. Metelitsa LS, Wu HW, Wang H, Yang Y, Warsi Z, Asgharzadeh S, et al. Natural killer T cells infiltrate neuroblastomas expressing the chemokine CCL2. J Exp Med 2004;199:1213–21.
15. Liu D, Song L, Wei J, Courtney AN, Gao X, Marinova E, et al. IL-15 protects NKT cells from inhibition by tumor-associated macrophages and enhances antimetastatic activity. J Clin Invest 2012;122:2221–33.
16. Tian G, Courtney AN, Jena B, Heczey A, Liu D, Marinova E, et al. CD62L+ NKT cells have prolonged persistence and antitumor activity in vivo. J Clin Invest 2016;126:2341–55.
17. Heczey A, Louis CU, Savoldo B, Dakhova O, Durett A, Grilley B, et al. CAR T cells administered in combination with lymphodepletion and PD-1 inhibition to patients with neuroblastoma. Mol Ther 2017;25:2214–24.
18. Long AH, Haso WM, Shern JF, Wanhainen KM, Murgai M, Ingaramo M, et al. 4-1BB costimulation ameliorates T cell exhaustion induced by tonic signaling of chimeric antigen receptors. Nat Med 2015;21:581–90.
19. Chen Y, Sun C, Landoni E, Metelitsa LS, Dotti G, Savoldo B. Eradication of neuroblastoma by T cells redirected with an optimized GD2-specific chimeric antigen receptor and interleukin-15. Clin Cancer Res 2019;25: 2915–24.
20. Matsuda JL, Gapin L, Sidobre S, Kieper WC, Tan JT, Ceredig R, et al. Homeostasis of V alpha 14i NKT cells. Nat Immunol 2002;3:966–74.
21. Baev DV, Peng XH, Song L, Barnhart JR, Crooks GM, Weinberg KI, et al. Distinct homeostatic requirements of CD4+ and CD4- subsets of Valpha24-invariant natural killer T cells in humans. Blood 2004;104:4150–6.
22. Keshelava N, Zuo JJ, Chen P, Waidyaratne SN, Luna MC, Gomer CJ, et al. Loss of p53 function confers high-level multidrug resistance in neuroblastoma cell lines. Cancer Res 2001;61:6185–93.
23. Seeger RC, Rayner SA, Banerjee A, Chung H, Laug WE, Neustein HB, et al. Morphology, growth, chromosomal pattern and fibrinolytic activity of two new human neuroblastoma cell lines. Cancer Res 1977;37:1364–71.
24. Ngai H, Tian G, Courtney AN, Ravari SB, Guo L, Liu B, et al. IL-21 Selectively Protects CD62L(+) NKT cells and enhances their effector functions for adoptive immunotherapy. J Immunol 2018;201:2141–53.
25. Vera J, Savoldo B, Vigouroux S, Biagi E, Pule M, Rossig C, et al. T lymphocytes redirected against the kappa light chain of human immunoglobulin efficiently kill mature B lymphocyte-derived malignant cells. Blood 2006;108:3890–7.
26. Roederer M, Nozzi JL, Nason MC. SPICE: exploration and analysis of post-cytometric complex multivariate datasets. Cytometry A 2011;79:167–74.
27. Song L, Asgharzadeh S, Salo J, Engell K, Wu HW, Sposto R, et al. Valpha24-invariant NKT cells mediate antitumor activity via killing of tumor-associated macrophages. J Clin Invest 2009;119:1524–36.
28. Lee PT, Benlagha K, Teyton L, Bendelac A. Distinct functional lineages of human V(alpha)24 natural killer T cells. J Exp Med 2002;195:637–41.
29. Ajina A, Maher J. Strategies to address chimeric antigen receptor tonic signaling. Mol Cancer Ther 2018;17:1795–815.
30. Maude SL, Frey N, Shaw PA, Aplenc R, Barrett DM, Bunin NJ, et al. Chimeric antigen receptor T cells for sustained remissions in leukemia. N Engl J Med 2014;371:1507–17.
31. Turtle CJ, Hanafi LA, Berger C, Gooley TA, Cherian S, Hudecek M, et al. CD19 CAR-T cells of defined CD4+:CD8+ composition in adult B cell ALL patients. J Clin Invest 2016;126:2123–38.
32. Kochenderfer JN, Dudley ME, Feldman SA, Wilson WH, Spaner DE, Maric I, et al. B-cell depletion and remissions of malignancy along with cytokine-associated toxicity in a clinical trial of anti-CD19 chimeric-antigen-receptor-transduced T cells. Blood 2012;119:2709–20.
33. Lee DW, Kochenderfer JN, Stetler-Stevenson M, Cui YK, Delbrook C, Feldman SA, et al. T cells expressing CD19 chimeric antigen receptors for acute lymphoblastic leukaemia in children and young adults: a phase 1 dose-escalation trial. Lancet 385:517–28.
34. Teachey DT, Rheingold SR, Maude SL, Zugmaier G, Barrett DM, Seif AE, et al. Cytokine release syndrome after blinatumomab treatment related to abnormal macrophage activation and ameliorated with cytokine-directed therapy. Blood 2013;121:5154–7.
35. Gomes-Silva D, Mukherjee M, Srinivasan M, Krenciute G, Dakhova O, Zheng Y, et al. Tonic 4-1BB costimulation in chimeric antigen receptors impedes T cell survival and is vector-dependent. Cell Rep 2017;21:17–26.
36. Crowe NY, Coquet JM, Berzins SP, Kyparissoudis K, Keating R, Pellicci DG, et al. Differential antitumor immunity mediated by NKT cell subsets in vivo. J Exp Med 2005;202:1279–88.
37. Conlon KC, Lugli E, Welles HC, Rosenberg SA, Fojo AT, Morris JC, et al. Redistribution, hyperproliferation, activation of natural killer cells and CD8 T cells, and cytokine production during first-in-human clinical trial of recombinant human interleukin-15 in patients with cancer. J Clin Oncol 2015;33:74–82.
38. Robinson TO, Schluns KS. The potential and promise of IL-15 in immuno-oncogenic therapies. Immunol Lett 2017;190:159–68.
39. Yu AL, Gilman AL, Ozkaynak MF, London WB, Kreissman SG, Chen HX, et al. Anti-GD2 antibody with GM-CSF, interleukin-2, and isotretinoin for neuroblastoma. N Engl J Med 2010;363:1324–34.
40. Sondel PM, Hank JA. Combination therapy with interleukin-2 and anti-tumor monoclonal antibodies. Cancer J Sci Am 1997;3Suppl 1:S121–S7.
41. Metelitsa LS, Gillies SD, Super M, Shimada H, Reynolds CP, Seeger RC. Antidisialoganglioside/granulocyte macrophage-colony-stimulating factor fusion protein facilitates neutrophil antibody-dependent cellular cytotoxicity and depends on FcgammaRII (CD32) and Mac-1 (CD11b/CD18) for enhanced effector cell adhesion and azurophil granule exocytosis. Blood 2002;99:4166–73.
42. Simon T, Hero B, Faldum A, Handgretinger R, Schrappe M, Niethammer D, et al. Consolidation treatment with chimeric anti-GD2-antibody ch14.18 in children older than 1 year with metastatic neuroblastoma. J Clin Oncol 2004;22:3549–57.
43. Ozkaynak MF, Gilman AL, London WB, Naranjo A, Diccianni MB, Tenney SC, et al. A comprehensive safety trial of chimeric antibody 14.18 with GM-CSF, IL-2, and isotretinoin in high-risk neuroblastoma patients following myeloablative therapy: children's oncology group study ANBL0931. Front Immunol 2018;9:1355.